The isotope effect and phase transitions in ammonium hexachloropalladate studied by neutron tunnelling spectroscopy

1999 J. Phys.: Condens. Matter 11 5483

(http://iopscience.iop.org/0953-8984/11/28/309)

J. Phys.: Condens. Matter **11** (1999) 5483–5495. Printed in the UK PII: S0953-8984(99)02729-0

The isotope effect and phase transitions in ammonium hexachloropalladate studied by neutron tunnelling spectroscopy

M Prager†, P Schiebel‡, M Johnson§, H Grimm†, H Hagdorn‡, J Ihringer‡, W Prandl‡ and Z Lalowicz‖

† Institut für Festkörperforschung, Forschungszentrum Jülich, D-52425 Jülich, Germany
‡ Institut für Kristallographie, Universität Tübingen, Charlottenstrasse 33, D-72070 Tübingen, Germany
§ Institut Laue–Langevin, F-38042 Grenoble Cédex, France
‖ H Niewodniczanski Institute of Nuclear Physics, Krakow, Poland

Received 17 March 1999, in final form 24 May 1999

Abstract. Above 30% deuteration, ammonium hexachloropalladate undergoes the phase transition $Fm3m \rightarrow P2_1/n$, with T_c increasing to 30.2 K for pure $(ND_4)_2PdCl_6$. Rotational tunnelling of NH_4 and NH_3D was used to study this phase transition. The transition energies are related to the tunnelling matrix elements h_i. NH_3D can be described as a one-dimensional rotor, with the one-dimensional matrix elements being almost exactly the averages of the three-dimensional ones. In the high-temperature phase the intensities of the respective tunnelling transitions confirm a statistical occurrence probability of the isomers. In the low-temperature phase the strength of the rotational potential increases by about 30%. A broadening of the NH_3D tunnelling line with decreasing temperature above the crystallographic phase transition is interpreted as an intermediate glass phase which evolves due to long-range dipolar coupling combined with positional disorder.

1. Introduction

Rotational potentials of ammonium ions in $(NH_4)_2BC_6$ compounds, with B a tetravalent metal ion and C a halogen, are systematically studied by tunnelling spectroscopy using neutrons [1, 2]. Ammonium hexachloropalladate, $(NH_4)_2PdCl_6$, is in this class the compound with the largest tunnel splitting. The crystal structure of the protonated species is $Fm3m$ down to helium temperature. The tunnelling sublevels are determined by the tetrahedral site symmetry of the ammonium ion. This leads to the well-known doublet at the transition energies $\hbar\omega_{A\rightarrow T} = 58\ \mu$eV and $\hbar\omega_{E\rightarrow T} \sim \frac{1}{2}\hbar\omega_{A\rightarrow T}$. In terms of tunnelling matrix elements this level scheme is described by just one single parameter, the 120° overlap matrix element h, since the four possibly different h_i are identical by symmetry and the three 180° overlap matrix elements H_i are negligibly small [3].

Because of its large tunnel splitting, $(NH_4)_2PdCl_6$ was seen as a candidate for showing the large isotope effect of rotational tunnelling. Very unexpectedly, however, $(ND_4)_2PdCl_6$ transforms into a new crystallographic low-temperature phase at $T_c = 30.2$ K [4]. In mixed crystals the phase transition temperature is expected to decrease with increasing degree of protonation until, at some critical concentration c_D^*, the phase transition is suppressed. The occurrence of the phase transition at such low temperature allows us to apply the very sensitive

0953-8984/99/285483+13$30.00

rotational tunnelling spectroscopy to investigate this phase transition characteristic of the perovskite A_2BC_6 family [5].

1.1. The effect of H/D mixing

A sample made of a mixture of purely protonated and purely deuterated material will contain—due to proton exchange—partially deuterated ammonium species. Since they are chemically equivalent they will occupy sites statistically. Accordingly, effects of disorder have to be considered. At low degrees of deuteration the predominant species are NH_3D and NH_4. Both show large tunnel splittings with reasonable intensities.

1.2. The phase transition

The phase transition in $(ND_4)_2PdCl_6$ leads from the high-temperature (HT) cubic phase $Fm3m$ to a low-temperature (LT) monoclinic phase $P2_1/n$ [6]. The most important change in the LT structure is a loss of any symmetry at the site of the ammonium ion accompanied by a large-angle rotation of the ammoniums and a small-angle rotation of $PdCl_6$ octahedra to new equilibrium orientations. The reduced site symmetry of the ammonium ion will be connected with a splitting of the T states. Due to the change of the environment of the ammonium ion at T_c, the rotational barrier and thus the size of the tunnel splitting will change, too. The large A $\rightarrow$ T tunnel splitting of the high-temperature phase allows for rather strong potential changes before the tunnel splitting of the LT phase is too small to be resolved in a high-resolution neutron scattering experiment. This makes the system very favourable for the intended study.

A similar sequence of phases to the one that occurs in the title compound is found for ammonium hexachloroplatinate. In this material the phase transition temperature of the deuterated compound is $T_c = 27.2$ K and the low-temperature crystal structure is $P4_2/n$ [7]. Despite the considerably stronger rotational potential of the ammonium ion, a deuteration-induced phase transition was observed in ammonium hexachloroplumbate at the higher temperature $T_c = 38.4$ K [8].

There are other ammonium compounds of the perovskite type known, where a transition occurs in the protonated material. $(NH_4)_2SeCl_6$ shows a phase transition at $T_c = 24.5$ K. The transition leads into a phase of unknown lower symmetry and a correspondingly complicated tunnelling spectrum [9].

2. Experimental procedure and results

2.1. Sample preparation

The sample preparation is based on $PdCl_2$ and ammonium chlorine as ingot materials. A problem with preparing A_2PdCl_6, A = NH_4^+ or ND_4^+, is due to the fact that the stable valence of Pd is Pd^{2+} and not Pd^{4+} as needed for the title compound. Only in an acid environment, i.e. when prepared under a flow of chlorine gas [10], does the synthesis lead to the required compound:

$$PdCl_2 + 2NH_4Cl + Cl_2 \rightarrow (NH_4)_2PdCl_6.$$

The degree of deuteration c_D is adjusted by choosing the appropriate ratio of NH_4Cl and ND_4Cl. In this way six samples have been obtained with nominal concentrations $c_D = 0$, 0.1, 0.3, 0.5, 0.7, 1. There was no extra control of the degree of deuteration in the final samples. However, the tunnelling spectra themselves allow an independent estimate of the actual degree of deuteration to be obtained: if the protons are distributed statistically among

the various isotopomers, their occurrence probability obeys a binomial distribution $p(n, c_D)$ and the proton density of a partially deuterated species is $np(n, c_D)$ (table 1, columns 2 to 5). This can be tested experimentally (see below).

Table 1. $np(n, c_D)$ for various c_D and all isotopomers with $n \neq 0$. $p(n, c_D)$ is the binomial distribution for finding a proton in the isotopomers NH_nD_{4-n}. The sum of all terms $np(n, c_D)$ yields the average number of protons of the ammonium ions at the given c_D. It is proportional to the total scattering probability of unit weight of the material.

Concentration	$I(NH_4)$	$I(NH_3D)$	$I(NH_2D_2)$	$I(ND_3H)$	T_c (K)
$c_D = 0.1$	2.62	0.87	0.10	0.00	—
$c_D = 0.3$	0.96	1.23	0.26	0.41	—
$c_D = 0.5$	0.25	0.75	0.75	0.25	18.0
$c_D = 0.7$	0.03	0.23	0.53	0.41	24.7
$c_D = 1.0$	—	—	—	—	30.2

2.2. Structural information

2.2.1. X-ray diffraction. To determine the phase transition temperature for the various degrees of deuteration, diffraction patterns of each sample were recorded as functions of temperature by an automized low-temperature x-ray diffractometer over the range $8 \leqslant T$ (K) $\leqslant 32$ while the sample was cooled down in a closed-cycle refrigerator with a temperature slope of about 4 K h^{-1}. Phase transition temperatures can be determined with an accuracy of about 1 K. Table 1 (last column) shows T_c obtained by this technique.

No phase transition is found for samples with $c_D \leqslant 0.3$. At $c_D = 0.5$, T_c has steeply increased to $\sim\frac{2}{3}$ of the value for the fully deuterated material (figure 1).

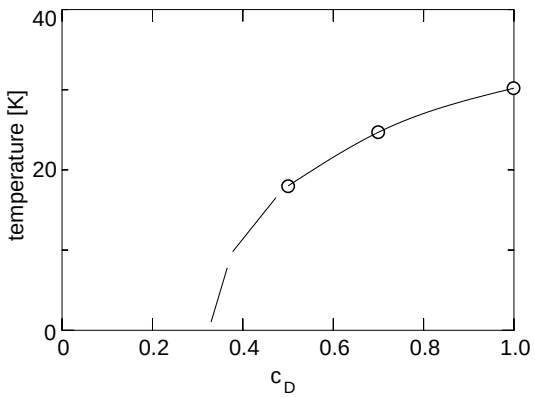

Figure 1. The variation of the temperature of the $Fm3m \rightarrow P2_1/n$ phase transition with deuteration c_D. The dashed curve is an extrapolation to low temperatures consistent with there being no phase transition below $c_D = 0.3$.

The HT cell volume at T_c amounts to about 918 Å^3. There is an increase of the LT cell volume at T_c of about 0.2%. The cell volume stays constant in the LT phase while it still decreases at the same temperature for concentrations where the phase transition does not occur [11].

2.2.2. Neutron diffraction. The space group of the low-T phase was determined using data taken at the neutron powder diffractometer D2b of the ILL, Grenoble. For $c_D \leqslant 0.3$ the structure remains cubic down to the lowest temperature $T = 4$ K as found in the x-ray experiment. The mixed crystals with $c_D \geqslant 0.5$ are monoclinic with space group $P2_1/n$ like the fully deuterated material [6]. Lattice parameters and cell volumes obtained from neutron diffraction coincide well with those derived from x-rays.

2.3. Inelastic neutron scattering

To cover the energy range -8 to 65 μeV, the high-resolution backscattering spectrometer IN10B of the ILL, Grenoble, was used with its KCl{200} variable-temperature monochromator at a wavelength $\lambda \simeq 6.27$ Å and energy resolution $\delta E \sim 2.0$ μeV. A typical measuring time for a complete spectrum was about 15 h. Finally, the maximum energy was reduced to about 30 μeV to get about 15 spectra in the range of sample temperatures $1.5\ K \leqslant T \leqslant 22$ K and deuterium concentrations $0.1 \leqslant c_D \leqslant 0.5$. The data at $c_D = 0.1$ were completed by spectra taken at the backscattering spectrometer BSJ at the research reactor FRJ2 of the FZ Jülich. The three spectra taken for $c_D = 0.5$ are characteristic of the high- and low-temperature phases and an intermediate situation; the sample with $c_D = 0.3$ undergoes significant changes of the NH_3D line profile despite the fact that it does not transform into the LT phase; similar features are observed for the sample with $c_D = 0.1$ with a denser net of temperature points (figure 2).

Transition energies are obtained by a standard fitting procedure. The scattering function is composed of an elastic line and tunnelling transitions. The former is represented by a δ-function and the latter by Lorentzians. The additional broad features are represented by Lorentzians, too. The scattering function composed this way is convoluted with the measured resolution function. Figure 3 shows the transition energies extracted this way; table 2 gives the numerical values. Some quantitative analysis is given in section 3.1.4.

3. Discussion

3.1. High-temperature (HT) and low-temperature (LT) phases

The spectrum of the HT phase, e.g. that for $c_D = 0.5$ and $T = 22$ K (figure 2), can be straightforwardly explained: the weak lines at 22.4/44.8 μeV represent the known T $\rightarrow$ E/A $\rightarrow$ T splitting of the librational ground state of the three-dimensional NH_4 rotor. The dominant new single line at 14.9 μeV is due to NH_3D species. The high occurrence probability of NH_3D explains its large intensity. The transition energy is close to that estimated by a rule of thumb from a potential strength scaling up the NH_4 potential using the ratio of the related rotational constants [12].

At $T = 2.0$ K the sample with $c_D = 0.5$ is in the LT phase. The strongest tunnelling line is now at $\hbar\omega_t = 7.2$ μeV (figure 2) and must be assigned—again due to its intensity—to the one-dimensional NH_3D rotor. The weak features at 10 μeV and above are assigned to NH_4 tunnelling. Thus all transitions are shifted to lower energies by about a factor of 2 due to stronger rotational potentials.

3.1.1. Scaling of tunnelling matrix elements in the high-T phase. For reasonably strong potential barriers the only important overlap matrix elements are those related to rotation about the four threefold axes (120° overlap h_i, $i = 1, \ldots, 4$). In the HT phase the molecular site symmetry is $\bar{4}$ and the four possible matrix elements are all identical and called h. If the zero of the energy scale is fixed to the unsplit T states of the ground state, the levels are [3, 13]

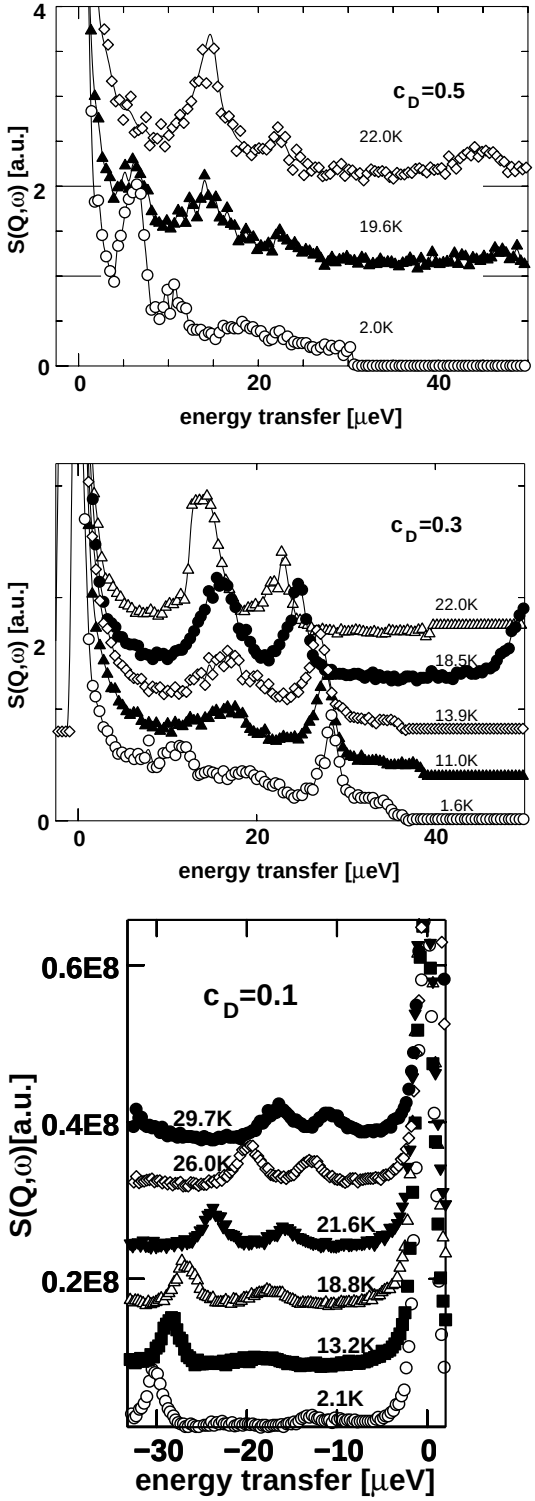

Figure 2. Tunnelling spectra of A_2PdCl_6, A = ammonium, at deuterations $c_D = 0.5$ and $c_D = 0.3$, instrument IN10B, ILL, and $c_D = 0.1$, instrument BSJ, FZ Jülich. At $c_D = 0.1$ and 0.3 the sample is in the HT phase at all temperatures.

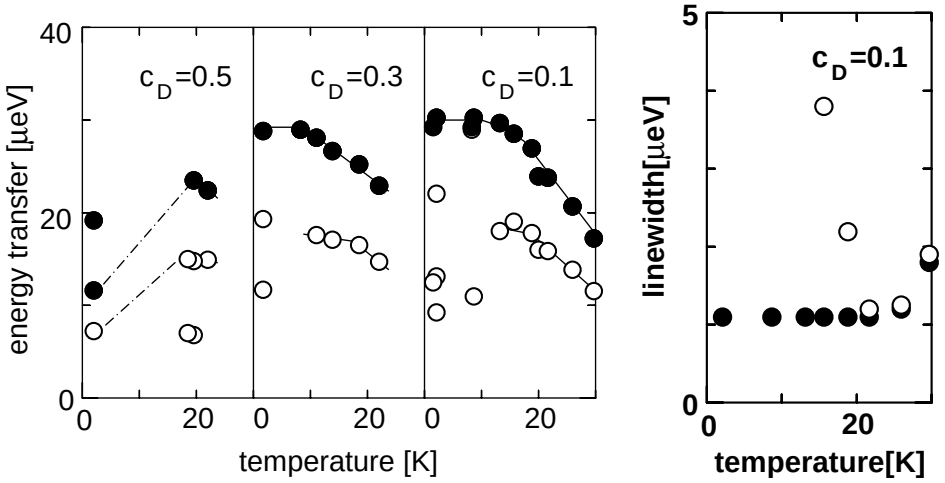

Figure 3. Sample: A_2PdCl_6, A = ammonium. The temperature dependence of the observed tunnel frequencies of the three partially deuterated samples investigated and linewidths for $c_D = 0.1$. Solid symbols refer to NH_4. Open symbols refer to NH_3D. The solid curves are guides to the eye.

$E(A\overline{A}) = 8h$, $E(T\overline{T}) = 0$, $E(E\overline{E}) = -4h$. Since h is negative, A is the tunnelling ground state. From the measured transition energy $\hbar\omega_{A\to T} = 58\ \mu$eV [4] one obtains $h = -7.25\ \mu$eV.

Partial deuteration reduces the symmetry of the potential. Due to the unique threefold axis of NH_3D, the one tunnelling matrix element h_1 exchanging only protons is distinct from and larger than the others, $h_1 \geqslant h_2 = h_3 = h_4$, and the energy levels become [3] $E(A\overline{A}) = 2h_1 + 6h_2$, $E(T\overline{A}) = 2h_1 - 2h_2$, $E(T\overline{E}) = -h_1 + h_2$, $E(E\overline{E}) = -h_1 - 3h_2$. h_2 is connected with a cyclic exchange of two protons and one deuteron.

Two procedures are proposed for estimating the parameter h_i from h obtained for the fully protonated species:

(a) The first recipe emphasizes the analogy to one-dimensional rotation. The rotational ground state in this case is a doublet. This is obtained mathematically from the above equations by choosing $h_2 = 0$. Physically the disappearance of h_2 is justified by the fact that h_2 describes the exchange of unequal atoms, H with D. The only sizable tunnel matrix element then is h_1. It describes the rotation about the threefold symmetry axis of the molecule. This tunnelling level scheme evolves from that of the original three-dimensional rotor when, at maximum splitting of the T states, one T state coincides with the A ground state the two others with the E level (cf. reference [3]). Under the assumption that the matrix element h_1 is unchanged, a tunnel splitting

$$\hbar\omega(NH_3D) = \frac{3}{8}\hbar\omega_{A\to T}(NH_4) = 21.75\ \mu\text{eV} \tag{1}$$

is calculated. The environment is assumed to remain tetragonal. The above equation can be rewritten as [3]

$$h_1 = \frac{1}{4}\sum h_i \tag{2}$$

which means that the one-dimensional tunnelling matrix element is just the average of the three-dimensional tunnelling matrix elements of the NH_3D species.

Due to the strange behaviour of the NH_3D tunnelling line, spectral features can only be compared at higher temperature in the mixed compound. For example, for $c_D = 0.1$

Table 2. The temperature dependence of the tunnelling transition energies $\hbar\omega$ (μeV) of partially deuterated ammonium hexachloropalladates. The linewidths are given in brackets. IN10B and BSJ are backscattering spectrometers at ILL and FZ Jülich, respectively, IN5 is the cold time-of-flight spectrometer of the ILL.

c_D	T (K)	NH_4		NH_3D			Instrument
0.0	3.6	58.1					IN5
	9.0	58.0					IN5
	16.2	54.4					IN5
	24.5	43.2					IN5
	28.3	37.2					IN5
	31.9	32.6					IN5
	35.1	29.0					IN5
0.1	1.5		29.2	19.3	11.7		IN10B
	8.3		29.0				IN10B
	20.0		23.9		16.0		IN10B
	2.1		29.1(1.1)	21.1	12.6	8.8	BSJ
	8.7		29.1(1.1)		10.6		BSJ
	13.2		28.5(1.1)	17.3			BSJ
	15.7		27.4(1.1)	18.2(3.8)			BSJ
	18.8		25.8(1.1)	17.1(2.2)			BSJ
	21.6		22.8(1.1)	15.2(1.2)			BSJ
	26.0		19.9(1.2)	13.2(1.2)			BSJ
	29.7	33.0	16.5(1.8)	11.0(1.8)			BSJ
0.3	1.5		28.8	19.3	11.7		IN10B
	8.3		29.0				IN10B
	11.0		28.1	17.6			IN10B
	13.9		26.8	17.1			IN10B
	18.5	50.3	25.2	16.5			IN10B
	22.0		22.9	14.8			IN10B
0.5	2.0	19.2	11.7			7.1	IN10B
	18.5			15		7.0	IN10B
	19.6	47.6	23.6	14.8		6.8	IN10B
	22.0	44.9	22.5	14.9			IN10B

and $T = 18.8$ K equation (1) yields

$$\hbar\omega(NH_3D) = 17.8\ \mu\text{eV} < \frac{3}{8} \times 26.9\ \mu\text{eV} = 20.2\ \mu\text{eV}.$$

The potential of the partially deuterated species is stronger than is predicted by extrapolation.

NH_4ClO_4 follows the same relation: the tunnel splitting of NH_3D in NH_4ClO_4 was found at $\sim$3.3 μeV [14]. Due to the m-plane at the ammonium site, the four possible orientations of NH_3D are inequivalent in this material: rotations about different rotational axes involve different tunnelling matrix elements h_i and thus lead to different tunnel splittings. However, the special values of the h_i [15] lead to a single triply degenerate somewhat broadened tunnelling line—found in the experiment—and an unresolved fourth one. The observed splitting is again smaller than the one calculated from equation (1): $\frac{3}{8} \times 2\sum h_i = 3.06\ \mu$eV. This means that, again, the barrier is stronger for the partially deuterated molecule.

Applied to NH_2D_2 the model makes all 120° overlap matrix elements very small and the tunnel splittings merge into the elastic line. This agrees with the fact that except

for almost free-rotor systems, e.g. Hofmann clathrates [16], ammonia on MgO [17] or methane [18, 19], rotational tunnelling around axes including an exchange of hydrogen and deuterium was never observed.

ND_3H has the same symmetry as NH_3D but the overlap matrix element h is much smaller and—since the proton is not involved in the particle exchange—the transition probability is weighted with the small incoherent scattering cross section of deuterium only. Thus a transition will be weak, and the energy transfer small. Despite the weak scattering, it might be technically possible to observe this transition at a large degree of deuteration c_D where protonated species are present with very low probability only. At such concentration our sample will transform into the tetrahedral phase, however.

(b) The second method is based on the isotope effect in rotational tunnelling. The argumentation follows from the Schrödinger equation of the problem [3]:

$$\left(-\nabla^2 + \frac{V}{B} - \frac{E_i}{B}\right)\Psi_i = 0. \tag{3}$$

∇^2 represents the dimensionless kinetic rotational energy, B is the rotational constant of the rotor, V the rotational potential, which is the product of a strength factor and a symmetry adapted normalized function (see the next section), and Ψ_i the eigenfunction of state i. At full deuteration the spatial symmetry of the problem is unchanged. However, the strength of the rotational potential is increased by the ratio of the rotational constants [3]. As regards rotational levels, both systems obey the same mathematical formalism and the tunnel splitting can be safely predicted from that of the protonated species. Maki [18, 20] had proposed interpolating the tunnel matrix elements of the partially deuterated isotopomers *despite the different symmetry* from the same formalism. On the basis of data on matrix-isolated methane, the matrix element h_1 is kept unchanged and h_2 calculated as the matrix element of a protonated species in a potential scaled up from that of the fully protonated species, the strength factor being called A_3 [13], by the ratio of the respective rotational constants B_x:

$$h_1(H_3)_{NH_3D} = h_1(H_3)_{NH_4}(A_3)$$
$$h_2(H_2D)_{NH_3D} = h_1(H_3)_{NH_4}\left(A_3\frac{B_{NH_4}}{B_{NH_3D}}\right).$$

From the symmetry ingredients of theory and intuition, it looks likely that the extrapolation to matrix elements exchanging equal particles may be correct while the generalization to an exchange of unequal atoms looks arbitrary for the strong rotational potentials considered in this paper. This view is supported by the fact that in none of the partially deuterated methyl groups, besides almost free rotors [16, 17, 19], was a tunnel splitting ever observed.

The quantitative treatment shows that the Maki procedure leads to nonzero tunnelling matrix elements of different size and thus to tunnelling spectra with split lines in disagreement with the experiment. The experiment supports the similarity of NH_3D tunnelling with one-dimensional rotation.

3.1.2. Rotational potentials. Barrier heights are calculated on the basis of the tunnel matrix elements of the three-dimensional rotor in a tetrahedral environment with a potential $V(\tau) = A_3 H_{11}^{(3)}(\tau)$ [13], where τ represents the quaternions and $H_{11}^{(3)}$ is the lowest-order symmetry-allowed cubic rotator function, and the exact solution of the Mathieu equation of the one-dimensional threefold rotor in a potential $V(\varphi) = (V_3/2)(1 - \cos(3\varphi))$. To compare the two phases, the system with $c_D = 0.5$ is considered. The results are given in table 3. If

the librational modes E_{01} were to be included, the potential shapes would need the inclusion of higher-order terms. In the case of NH_4, the corresponding mathematics is not available; in the case of NH_3D, E_{01} is not known.

Table 3. Potential barriers of NH_3D and NH_4 rotors for $c_D = 0.5$ as estimated from the tunnel splittings observed.

$\hbar\omega$ (μeV)	Species	Phase	Potential, B
19*	NH_3D	$Fm3m$	$V_3 = 38$
7.2	NH_3D	$P2_1/n$	$V_3 = 50$
29/58*	NH_4	$Fm3m$	$A_3 = 50$
10/20	NH_4	$P2_1/n$	$A_3 = 66$

* Extrapolated to zero temperature on the basis of the temperature dependence observed for the samples not showing a structural phase transition; $c_D \leqslant 0.3$.

The shift of the NH_3D tunnelling line is related to an increase of the strength of the rotational potential from $V_3 = 38B$ to $50B$. On scaling A_3 by the same factor $66B$, the tunnelling pattern of the three-dimensional NH_4 rotor in the new environment is estimated to be $\hbar\omega_{ET} = 10$ μeV and twice that value for the A $\rightarrow$ T transition. There does indeed exist such a doublet of lines (figure 2). The increased width of these lines must be related to T-state splittings at the lower site symmetry.

Investigating rotational tunnelling as a function of pressure has shown [4] that the potential barrier of the ammonium ion in $(NH_4)_2PdCl_6$ and thus the intermolecular interaction $V(r)$ increases with intermolecular distances r as $r^{-11\pm2}$. The observed change of tunnelling frequency at the phase transition would thus involve a linear contraction by 2.5%. The diffraction experiment shows, however, that the volume of the unit cell increases at T_c by 0.2%. The crystallographic parameters [6, 11] show that the packing of nearest neighbours changes significantly due to the large-angle reorientation of the ammonium ion. Correspondingly, the unique distance of hydrogen atoms from the nearest chlorine ions of 2.9 Å in the HT phase becomes different and some as short as 2.4 Å. Thus it is probably not the average interatomic distance but the reduced distance to the nearest neighbours which creates the increased rotational potential of the LT phase.

3.1.3. Intensities. In the high-temperature cubic phase all theoretical information is available for quantitative analysis of the spectra. The scattering function of the three-dimensional tetrahedral rotor (NH_4) normalized to the scattering of one proton is [3]

$$S(Q,\omega) = \left(\frac{7}{4} + \frac{9}{4}j_0\right)\delta(\omega) + \frac{5}{8}(1 - j_0)\delta(\omega \pm \omega_{AT}) + \frac{4}{8}(1 - j_0)\delta(\omega \pm \omega_{ET}). \tag{4}$$

Similarly the normalized scattering function of a one-dimensional threefold rotor (NH_3D) is

$$S(Q,\omega) = \left(\frac{5}{3} + \frac{4}{3}j_0\right)\delta(\omega) + \frac{2}{3}(1 - j_0)\delta(\omega \pm \omega_t). \tag{5}$$

The spherical Bessel function j_0 appears in the structure factors due to orientational averaging.

Thus, if the occurrence of the various isotopic species is random, $p(n, c_D)$, then the ratio of intensities of the respective transitions is

$$\frac{S(Q,\omega_t)}{S(Q,\omega_{ET})} = \frac{4}{3}\frac{p(3,c_D)}{p(4,c_D)}. \tag{6}$$

Figure 4 includes also literature results from other experiments like those described in [14]. It shows that this relation is indeed fulfilled at all degrees of deuteration. It tells us also

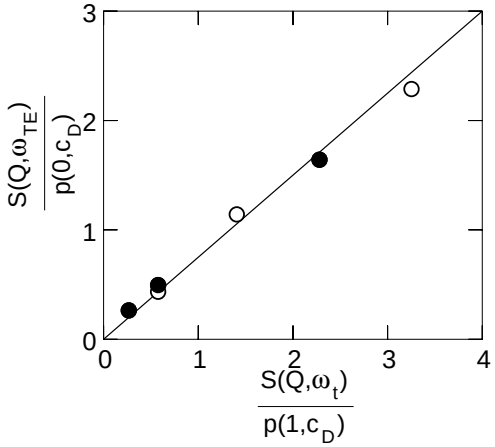

Figure 4. The three-dimensional tunnelling structure factor normalized to the occurrence probability of NH_4 ions plotted versus the one-dimensional tunnelling structure factor normalized to the occurrence probability of NH_3D. The solid line shows the theoretically expected ratio. Full symbols: this experiment; open points: reference [14].

immediately that all samples had the claimed degree of deuteration. The assignment of the tunnelling transitions in the high-temperature phase is thus fully confirmed by the line intensities, and proton sites are occupied by H/D statistically. This latter has to be emphasized, since it has been claimed that deviations from full exchange have been seen in an ammonia compound [16].

3.1.4. Linewidths. The shift and broadening of tunnelling lines with temperature is caused by coupling to phonons and follows Arrhenius laws [21]:

$$\Delta\hbar\omega_t(T) \sim \exp\left(-\frac{E^{\mathrm{S}}}{kT}\right)$$

$$\Gamma(T) \sim \exp\left(-\frac{E^{\Gamma}}{kT}\right).$$

The broadening is due to resonant coupling to phonons of the single-particle librational energy and thus $E^{\Gamma} = E_{01}$, while the shift involves coupling to all low-energy phonons and thus $E^{\mathrm{S}} < E_{01}$. The simplest spectra of the fully protonated material allow this analysis (figure 5).

Since there is a low density of states below E_{01}, one would expect $E^{\mathrm{S}} = E^{\Gamma} = E_{01}$. The broadening was too weak to be measured. Given the measured librational energy of $E_{01} = 5.8$ meV [4], $E^{\mathrm{S}} = 5.2$ meV is indeed only a little smaller.

With deuteration, the phase transition is expected to influence the temperature dependence of the tunnelling sublevels. This is based on the general property of second-order phase transitions being driven by the softening of a characteristic mode whose eigenvector has the same symmetry as the final distortion.

In the case of the very thoroughly investigated cubic $\rightarrow$ tetragonal transition of A_2BC_6 compounds, the characteristic mode is a libration of the BC_6 octahedra around the future tetragonal axis. The atoms at the corner of this octahedron are nearest neighbours of the protons of the ammonium group and largely determine the strength of the rotational potential. The critical slowing down of this mode at T_c offers a new possibility for studying the interaction of a tunnelling rotor with phonons: instead of populating all phonon states with increasing sample

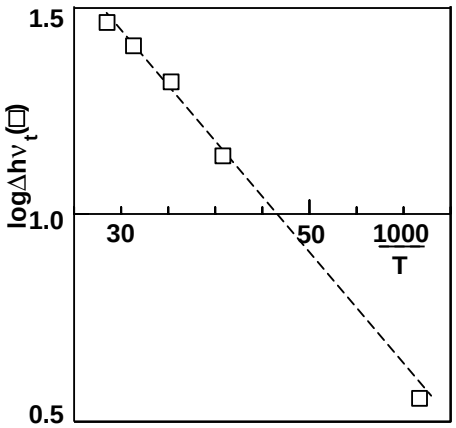

Figure 5. An Arrhenius plot of the shift of the tunnelling lines of ammonium ions in $(NH_4)_2PdCl_6$. Energies are in μeV, temperatures in K.

temperature, one special phonon is *populated selectively at decreasing sample temperature* due to the softening of the related eigenmode. At the same time the librational mode probably shifts as a result of the changing environment and thus coupling to phonons is modified. However, since the line *broadening with decreasing temperature*, i.e. with $T - T_c$ approaching zero (figure 2; $c_D = 0.1$), is only seen for the NH_3D species, its origin is more probably an inhomogeneous broadening due to disorder (see the next section).

3.2. The dipolar glass phase

The most surprising observation concerns the different behaviour of NH_3D and NH_4 molecules on changing the temperature (figure 2; linewidth). The occurrence probability of the two species is stable; they occupy crystallographically equivalent sites. Despite all of these similarities, there is a temperature regime where the one-dimensional NH_3D rotor becomes spread out over a wide energy range while the doublet of the tunnelling NH_4 molecules remains almost unchanged (figure 3; linewidth). In the generally used local single-particle model this means that, contrary to expectation, the rotational potential of the NH_3D rotor changes very differently to that of NH_4. This intermediate regime is best seen at low degrees of deuteration, $c_D \leqslant 0.3$, where a structural phase transition could not be detected.

There is no quantitative explanation of this observation yet. The reason for this behaviour has been searched for in different properties of NH_4 and NH_3D and the disorder of mixed crystals. Experience with other systems with disorder, like rubidium ammonium dihydrogen phosphate [22] and argon/nitrogen [23], shows that mixed systems with different crystallographic structures of the pure compounds often form glassy low-temperature phases at intermediate concentrations.

A material very closely related to our system is mixed $(KI)_{1-x}(NH_4I)_x$. In this system the discrepancy between molecular and site symmetry leads to a tilted orientation of the ammonium ion with one distinguished N–H$\cdots$I bond. The polarization of the environment creates an induced dipole moment. The corresponding long-range interaction in combination with occupational disorder leads to an orientational dipolar glass phase at around $x \geqslant 0.17$ [24, 25]. With $d_{AA} \sim 5$ Å, distances between ammonium ions are much larger in ammonium hexahalo-compounds than in NH_4I. The octupole–octupole interaction between them is rather localized,

$\sim r^{-7}$, and does not influence the ammonium rotational potential appreciably [26]. The situation becomes different for NH_3D. Due to its lower symmetry, the molecule represents a dipole with long-range interaction with other ammoniums. The relative importance of dipole–dipole interaction with respect to octupole–octupole interaction increases as $\sim r^4$ and thus a factor $\sim$600 at the nearest ammonium–ammonium distance $d_{AA} \sim 5$ Å. Its absolute value requires a knowledge of the dipole moment. Due to the lack of experimental data we estimate the dipole moment of NH_3D from the assumption that the centre of mass of the molecule coincides with the crystallographic site, while the centre of charge, on the other hand, is still the geometric centre of the molecule. This leads to an off-centre position with a displacement of $\sim$0.055 Å. For a fixed environment the centre of the negative charge is unchanged. Assuming a full positive and a full negative charge for the ammonium ion and the environment, respectively, the dipole moment is $\sim 0.1D$. For this dipole moment the dipole–dipole energy at the intermolecular distance d_{AA} is, in temperature units, about $20k$, k being the Boltzmann constant. In a temperature regime where the lattice shows an instability, this weak additional interaction can enable the NH_3D ion to flip along the soft direction of the potential to new equilibrium orientations which are probably close to those of the final LT crystallographic phase. The statistical occupation of ammonium sites by NH_3D molecules must lead to orientational disorder in a glass-like phase. The fluctuation of the rotational barrier should be of the order of the dipolar interaction, i.e. 10% of the basic potential. A rough estimate shows that the corresponding line broadening is then some μeV, in accordance with observation.

NMR techniques are generally able to detect subtle motions of ammonium ions such as the small-angle reorientational jumps around the symmetry axes in some other perovskites [27]. It looks difficult, however, to characterize the complex and distinct behaviour of the various isotopic ammonium species in the weak rotational potential of our partially deuterated compound by NMR lineshape experiments. More detailed calculations and further experiments along the lines discussed in reference [25] have to be performed before a consistent quantitative description of this interesting system can be given.

4. Summary and conclusions

Ammonium palladium hexachloride belongs to the group of systems for which quantum mechanical differences between the protonated and deuterated species drives a deuteration-induced phase transition at very low temperatures. The structural phase transition appears at a partial deuteration just above $c_D = 0.3$.

High-resolution neutron tunnelling spectroscopy of the librational ground state of the ammonium ions is used to study the system around the phase transition. Partial deuteration is reflected in the presence of all types of partially deuterated ammonium species. Neutron scattering is sensitive to NH_4 and NH_3D. Tunnelling spectra can be explained quantitatively as superpositions of single-particle rotational transitions and under the assumption that NH_3D undergoes one-dimensional tunnelling about its symmetry axis. Its 1D tunnelling matrix element is simply the average of the 3D tunnelling matrix elements. (A scaling of tunnelling matrix elements as proposed for methane [20] fails.) The ratio of the intensities of the tunnelling lines due to NH_4 and NH_3D shows that H/D exchange is complete: the ammonium occurrence probabilities are binomial.

On transformation into the low-temperature phase the tunnelling energy is diminished, according to the increase of the rotational barrier by about 30%.

While the NH_4 tunnelling lines within a phase change with temperature according to the established theory [21], the NH_3D lines already significantly broaden with decreasing

temperature above T_c. We interpret this phenomenon as inhomogeneous broadening: dipolar interaction between NH_3D species and positional disorder is supposed to lead to a dipolar glass state. The observed tunnelling line then represents the envelope of many weakly different tunnelling states.

Acknowledgments

We thank Dr Herma Büttner and Dr A Ritter for the help with experiments.

References

[1] Prager M, Raaen A M and Svare I 1983 *J. Phys. C: Solid State Phys.* **16** L181
[2] Prager M and Heidemann A 1997 *Chem. Rev.* **97** 2933
[3] Press W 1981 *Single Particle Rotations in Molecular Solids (Springer Tracts in Modern Physics vol 82)* (Berlin: Springer)
[4] Prager M, Press W, Heidemann A and Vettier C 1983 *J. Chem. Phys.* **80** 2777
[5] Winter J and Roessler K 1980 *Phys. Rev.* B **21** 2920
[6] Swainson I P, Powell B M and Weir R D 1997 *J. Solid State Chem.* **131** 221
[7] Yamamuro O, Okishiro K, Matsuo T, Onoda-Yamamuro N, Oikawa K, Kamiyama T, Kume Y and Izumi F 1997 *J. Chem. Phys.* **107** 8004
[8] Kume Y, Muraoka H, Yamamuro O and Matsuo T 1998 *J. Chem. Phys.* **108** 4090
[9] Arnscheidt J and Pelzl J 1998 unpublished
[10] Brauer G 1962 *Handbuch der Präparativen Anorganischen Chemie* 2nd edn, vol 2 (Stuttgart: Enke) p 1379
[11] Schiebel P, Ritter H H, Ihringer J, Prandl W and Prager M 1999 to be published
[12] Ozaki Y, Maki K, Okada K and Morrison J A 1985 *J. Phys. Soc. Japan* **54** 2595
[13] Hüller A and Raich J 1979 *J. Chem. Phys.* **71** 3851
[14] Büttner H, Kearley G J and Frick B 1997 *Chem. Phys.* **214** 425
[15] Prager M and Press W 1981 *J. Chem. Phys.* **75** 494
[16] Wegener W, Bostoen C and Coddens G 1990 *J. Phys.: Condens. Matter* **2** 3177
[17] Havighorst M, Prager M and Carlile C 1994 *Physica* **202** 355
[18] Lushington K J, Morrison J A, Maki K, Heidemann A and Press W 1983 *J. Chem. Phys.* **78** 383
[19] Asmussen B, Prager M, Müller M, Balszunat D, Press W and Carlile C J 1996 *J. Chem. Phys.* **105** 1763
Asmussen B, Balszunat D, Press W, Prager M, Carlile C J and Büttner H 1994 *Physica* B **202** 224
Asmussen B, Balszunat D, Press W, Prager M, Carlile C J and Büttner H 1995 *J. Chem. Phys.* **103** 6880
[20] Maki K 1981 *J. Chem. Phys.* **74** 2049
[21] Hewson A C 1982 *J. Phys. C: Solid State Phys.* **15** 3841
Hewson A C 1982 *J. Phys. C: Solid State Phys.* **15** 3855
[22] Parlinski K and Grimm H 1986 *Phys. Rev.* B **33** 4868
[23] Press W, Janik B and Grimm H 1982 *Z. Phys.* B **49** 9
[24] Bostoen C, Coddens G and Wegener W 1989 *J. Chem. Phys.* **91** 6337
Fehst I, Böhmer R, Ott W, Loidl A, Haussühl S and Bostoen C 1990 *Phys. Rev. Lett.* **64** 3139
[25] Berret J-F, Bostoen C and Hennion B 1992 *Phys. Rev.* B **46** 13 747
[26] Prager M, Press W and Roessler K 1980 *J. Mol. Struct.* **60** 173
[27] Dimitropoulos C and Lalowicz Z 1994 *Phys. Rev.* B **49** 644